Ecological Engineering 185 (2022) 106811

Contents lists available at ScienceDirect

Ecological Engineering

journal homepage: www.elsevier.com/locate/ecoleng

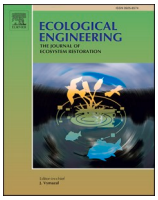

Tree root distribution modelling in different environmental conditions

Paolo Perona [a,*], Reto Flury [b], D. Andrew Barry [c], Massimiliano Schwarz [d]

[a] Hydraulic Constructions Platform (PL-LCH), Institute of Civil Engineering (IIC), School of Architecture, Civil and Environmental Engineering (ENAC), École polytechnique fédérale de Lausanne (EPFL), Lausanne 1015, Switzerland
[b] HOLINGER AG, Urban Drainage and Hydraulic Engineering, Kasthoferstrasse 23, Bern CH-3000, Switzerland
[c] Ecological Engineering Laboratory (ECOL), Institute of Environmental Engineering (IIE), School of Architecture, Civil and Environmental Engineering (ENAC), École Polytechnique Fédérale de Lausanne (EPFL), Lausanne 1015, Switzerland
[d] Forestry Department, Bern University of Applied Sciences, Länggasse 85, Zollikofen 3052, Switzerland

ARTICLE INFO

2000 MSC:
0000
1111
PACS:
0000
1111
Keywords:
Root distribution model
Below-ground biomass
Root system area
Riparian vegetation
Plant root modelling
Ecohydraulics
Ecohydrology

ABSTRACT

The ability to predict the spatial distribution of tree root system variables (e.g., the Root system Area (RA), the maximum root diameter, the number of roots in diameter classes, the density of fine roots, etc.) under different environmental conditions is relevant to several scientific disciplines and to engineering practice. In this work, three well known analytical models from the literature are assembled into a unique framework called the Root Distribution Model (RDM). RDM models the expected vertical and horizontal distribution of coarse and fine root system variables for mature plants growing in different environmental conditions ranging from moderately humid to arid climates. All soil and moisture dynamic parameters are physically based, which make the model straightforward to calibrate via a single tuning parameter. At this investigative stage, it is shown that the model has the flexibility to represent a broad range of situations where soil moisture may result from precipitation inputs or from water level fluctuations due to either the presence of a water coarse or of deep aquifers or both. Accordingly, the distribution of the sectional RA may be either positively or negatively skewed, as well as show a peculiar bi-modal structure. The model can be used to study the impact of changing scenarios affecting precipitation, aquifer and channel hydrology.

1. Introduction

Mathematical modelling of bio- and ecomorphodynamic processes in catchment slopes and fluvial systems has considerably advanced with the inclusion of flow and vegetation interaction dynamics (Camporeale et al., 2013; Gasser et al., 2019). Although research is ongoing, the role that vegetation above- and below-ground biomass plays in such dynamics is also key for ecological and civil engineering applications. Vegetation contributes to all hydrogeological catchment processes including regulating the water budget at a point (Rodrigez-Iturbe and Porporato, 2005), controlling bank and bed erosion of river channels (Thorne, 1990; Abernethy and Rutherfurd, 2001), influencing slope stability in the catchment headwaters as well as triggering of mass movements (e.g., snow, mud, rock and debris in general, e.g. see Gasser et al. (2019); Reubens et al. (2007)). Modelling the distribution of vegetation roots is relevant to understand whether and how plant roots contribute to the mechanical reinforcement of soil on slopes (hence, slope stabilization (Schwarz et al., 2010b; Ennos and Pellerin, 2000; Stokes, 2002)), and to forecast when uprooting by flow occurs (Edmaier et al., 2011, 2015; Perona and Crouzy, 2018). In turn, this allows for assessment of the amount of potentially transportable wood biomass to downstream river sections (Gasser et al., 2019; Ruiz-Villanueva et al., 2016; Wohl and Scott, 2017) and for calculation of the probability that wood accumulation may choke the stream (Schalko et al., 2020). Hence, the provision of model-based theory is useful for calculation of the exposure risk to natural hazards of the natural and the built environments.

Modelling plant root growth and the related spatial distribution has been the object of several previous investigations. Both very detailed 3D explicit models (e.g., see Postma et al. (2017)) and simplified, physically-based (either laterally or vertically integrated) 1D models exist. Whilst the first are typically useful to investigate water uptake and the biomorphology and architecture of roots, their complexity is often unnecessary and excessively costly computationally (Schwarz et al., 2010a). For practical applications including the creation of spatial hazard maps (e.g., see Gasser et al. (2019)), 1D models providing

* Corresponding author.
E-mail address: paolo.perona@epfl.ch (P. Perona).

https://doi.org/10.1016/j.ecoleng.2022.106811
Received 30 December 2021; Received in revised form 20 September 2022; Accepted 29 September 2022
Available online 19 October 2022

analytical formulas for either the lateral root distribution (Schwarz et al., 2010a, 2012) or the vertical root profile (Laio et al., 2006; Tron et al., 2014) are more suitable. Such models are parameterized with physically-based (and commonly measured) soil, hydrological and biological variables. However, progress is still required to make such models fully accessible in practice. A great improvement would be to develop a joint 2D model able to provide both the vertical and the lateral distributions of common tree root variables, including the sectional Root system Area (hereafter referred to as RA, see Fig. 1) thus representing more realistic estimates of the soil biomass distribution. First of all, such a model would allow study of the role of environmental variables, such soil moisture and texture, hydrology, groundwater, etc., in a more comprehensive and integrated way. Furthermore, by linking the RA to the mechanical reinforcement of the soil, the model could then be implemented as an additional module of existing bank erosion models at the river cross-section (e.g., BANKforNET, see Gasser et al. (2020) or BSTEM, see Pollen-Bankhead and Simon (2009)) and the reach scales (e.g., BANKforMAP, see Gasser (2020)).

In this work, three existing 1-D plant root models are linked into a single 2D modelling framework, which provides the explicit distribution of the below-ground biomass variables along the lateral (horizontal) and the vertical (depth) directions. The 1D models are those Schwarz et al. (2010a, 2012), Laio et al. (2006) and Tron et al. (2014, 2015), whose main characteristics are hereafter briefly reviewed.

The model of Schwarz et al. (2010a) is symmetrical around the vertical and provides the vertically integrated distribution of root geometrical variables (e.g., diameter, cross-section area, etc.) as a function of the lateral distance from the tree stem centerline, up to a maximal distance of growth. Root architecture statistics are linked to the distribution of fine roots via a fractal branching geometry model, and depend on the total biomass distributed around a circular cylinder of unitary soil depth. Eventually, the total biomass is parameterized as a function of macroscopic above-ground biomass quantities through allometric relationships, which is very convenient for rescaling purposes and building a linked framework. The model of Laio et al. (2006) describes the stochastic dynamics of the soil moisture at a point. It accounts for moisture uptake due to root biomass as it varies with depth.

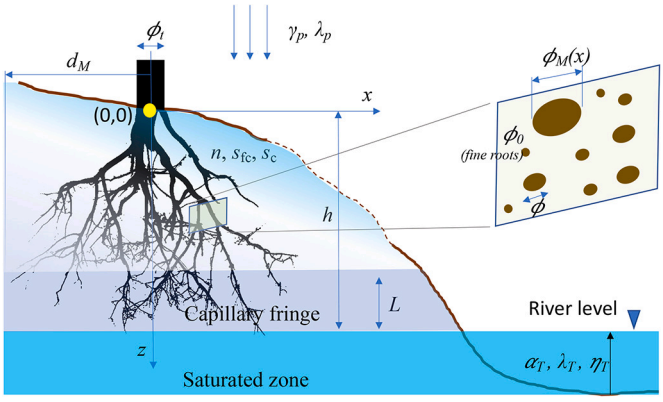

Fig. 1. Scheme of the model variables. The yellow dot indicates the origin of the coordinates $(x, z) = (0, 0)$, which is coincident with top soil elevation where the tree grows. The model variables are explained in the text, whereas the zoomed cross-section shows the RA as the sum of the brown areas of all coarse roots with diameter $\phi_0 < \phi \leq \phi_M$ within the section at lateral coordinate x. The uniform cyan zone indicates the watertable (upper limit of the saturated zone, water pressure is atmospheric), the light dark blue zone is the capillary fringe (water pressure is less than atmospheric) available for root growth as in the Tron et al. (2014) model, the upper non-uniform light cyan zone indicates where soil moisture recharge occurs via rainfall as per the Laio (2006) model. As shown in the figure, fluctuations in the river level drive fluctuations in the watertable level. (For interpretation of the references to colour in this figure legend, the reader is referred to the web version of this article.)

At statistical equilibrium, the model relates the vertical root biomass distribution, $r(z)$, to soil (e.g., porosity) and climatic conditions (e.g., rainfall and temperature) via the Budyko climate index (Dingman, 2002). Both models, however, do not consider the role of watertable oscillations and are therefore of limited use for describing root growth in the vicinity of water courses (the case of riparian plants, for instance). This can be achieved by appealing to the model of Tron et al. (2014), which provides the statistical equilibrium solution of the vertical root profile under the effect of stochastic fluctuations of river levels, and dichotomic root growth and recession dynamics (see also Ridolfi et al. (2011)). This model was shown to agree well with data from both field and laboratory experiments (e.g., see Tron et al. (2015)), and thus provides the ideal missing modelling framework to describe the effect of groundwater fluctuations on the vertical root profile.

Common to the three models is the provision of the statistical distribution of plant root biomass-related quantities at their mature stage, which are complementary and not redundant. Consequently, the models can be combined into a unified framework. In the next Section, the main equations of each model are presented and then recast to build the Root Distribution Model. Section 3 presents results and then explores the potential of the model, highlighting novel features of this new modelling framework. Section 4 presents conclusions.

2. Mathematical frameworks and the root distribution model

2.1. Framework models description

We start by considering the model of Schwarz et al. (2010b, 2012) in the scheme shown in Fig. 1. Defining the lateral distance from the tree stem as x, Schwarz et al. (2012) obtained the number of roots, $N(\phi, x)$, as a function of x and the root diameter class size, ϕ, as

$$N(\phi, x) = D_{fr}\frac{ln(1+\phi_M) - ln(1+\phi)}{ln(1+\phi_M)}\left(\frac{\phi}{\phi_0}\right)^{\lambda_r}, \tag{1}$$

which is valid for $\phi_t/2 \leq x \leq d_M$ and $\phi_0 < \phi \leq \phi_M$. At a given radial distance, $x = d_{lim}$, the maximum root diameter, ϕ_M, is equal to ϕ_0, which is a reference diameter (usually assumed to be 1 mm, see Schwarz et al. (2012)) below which roots are classified as fine roots. The maximum rooting distance, d_M, is generically parameterized as a function of the trunk Diameter at Breast Height (DBH), here indicated by ϕ_t, whereas λ_r is an empirical exponent according to (Schwarz et al., 2012). It is assumed $d_M = a_0\phi_t$, where a_0 is simply a proportionality constant depending on tree species. D_{fr} is the density of fine roots, which are a key reference quantity used in below-ground biomass investigations given their key role in uptaking water and nutrients from soil (Stokes, 2002; Smith, 2007). The density of fine roots is also a function of the distance x from the trunk and assumed to have the following stepwise distribution function

$$D_{fr}(x) = \frac{\mu\phi_t}{2\pi d_M}\left(\frac{1}{5\phi_t}\left(0.7 + 0.3\frac{x}{5\phi_t}\right)\Theta[5\phi_t - x] + \frac{1}{x}\Theta[x - 5\phi_t]\right), \tag{2}$$

where $\Theta[\cdot]$ is the Heaviside function and μ is a pipe-theory coefficient. Notice that this distribution normalizes the total number of fine roots to the cylinder of circumference radius x and unitary depth. As above, the distribution is defined in the domain $\phi_t/2 \leq x \leq d_M$.

Finally, the maximum diameter of roots at a given distance is taken as the result of fractal branching trees involving the branching distance b and the reference cross-sectional area A_{fr} of fine roots with diameter ϕ_0, i.e. $A_{fr} = \pi/4\ mm^2$. ϕ_M changes with the distance from the stem as

$$\phi_M(x) = s\frac{d_M - x}{b}A_{fr}\Theta[d_M - x], \tag{3}$$

where s is a scaling factor. This relation is defined in the range $\phi_t/2 \leq x \leq d_{lim}$, where $d_{lim} = d_M - \phi_0 b/sA_{fr}$, which is the radial distance where

$\phi_M(d_{lim}) = \phi_0$ (see also Schwarz et al. (2012) for details).

The model of Laio et al. (2006) provides the expected vertical (i.e., along z) root biomass probability density function (pdf) as analytical solutions of a point water balance stochastic model. For semi-arid and arid climatic conditions, if precipitation magnitude is exponentially distributed with mean γ_p and occurs as a Poisson stochastic process of rate λ_p, then Laio et al. (2006) predicts that the pdf of roots, $r_L(z)$, is also exponential

$$r_L(z) = \frac{1}{b_L} exp(-z/b_L). \tag{4}$$

In this relationship, $b_L = \gamma_p/A$ is the mean rooting depth, whereas A is a nondimensional value that depends on soil, plant and climate characteristics:

$$A = n(s_{fc} - s_w)\left(1 - \frac{1}{D_I}\right). \tag{5}$$

where n is soil porosity, s_{fc} is soil moisture content at field capacity, s_w is the soil moisture triggering the wilting conditions in plant leaves and D_I is the Budyko index of climatic conditions, given by

$$D_I = \frac{T_p}{\lambda_p \gamma_p}, \tag{6}$$

with T_p, being the mean potential evapotranspiration during the growing season. The exponential solution for $r_L(z)$ is derived under the hypothesis that hydrotropism is the dominant factor and therefore roots optimally grow where water availability is higher. This condition is valid for moderate humid to arid conditions, but it may becomes a strong limiting assumption for very humid environments (e.g., tropics).

The model of Tron et al. (2014) provides the vertical root biomass distribution in response to river level oscillations. That is, the model describes how plants develop roots in the riparian zone where groundwater responds promptly to river level fluctuations. Moreover, in the model water is assumed to be available for uptake from roots only within the capillary fringe zone, which is subject to negative pore-water pressure. Whilst referring the reader to Tron et al. (2014) for mathematical details, here it suffices to say that river level variability is assumed to follow a Compound Poisson Process (Ridolfi et al., 2011) of rate λ_T, rate of exponential decay η_T, and mean jump magnitude α_T. Above the watertable, the capillary fringe has moisture available to roots within a window of amplitude L. The vertical motion of the capillary fringe follows the river level fluctuations so that roots can grow during the periods when they are inside the band L or die if they are outside of it. This"switching" dynamic is also stochastic and follows the so-called Dichotomous process (Ridolfi et al., 2011), where the switch between growth and death depends on periods of wetness and dryness. The model possesses only physically-based parameters and the solution for the vertical root profile, $R_T(z)$, reads as

$$R_T(z) = \frac{2\theta(z)k(z)}{\theta(z) + \theta(z)k(z) + 1 - k(z)}. \tag{7}$$

where $\theta(z)$ is the ratio between root growth and decay rates, which varies with the depth z from the surface (positive downward). $\theta(z)$ is assumed to be decreasing with z to describe the difficulty of plants to develop roots at greater depths. The function $k(z)$ is given by

$$k(z) = \begin{cases} \left[\Gamma\left(\widetilde{\lambda}_T, \frac{h-z-L}{\alpha_T}\right) - \Gamma\left(\widetilde{\lambda}_T, \frac{h-z}{\alpha_T}\right)\right]\Gamma\left(\widetilde{\lambda}_T\right)^{-1} & \text{if } -\infty < z < h-L, \\ 1 - \Gamma\left(\widetilde{\lambda}_T, \frac{h-z}{\alpha_T}\right)\Gamma\left(\widetilde{\lambda}_T\right)^{-1} & \text{if } h-L < z < h, \end{cases} \tag{8}$$

where $\Gamma(\cdot)$ is the gamma function and $\Gamma(\cdot,\cdot)$ is the incomplete gamma function. According to Tron et al. (2014) and Tron et al. (2015), the parameters h and L depend on plant and soil characteristics, in particular, h represents the soil depth below which roots do not grow due to persistent saturated conditions and so coincide with the minimum river level. The parameter $\widetilde{\lambda}_T$ is the ratio between the mean frequency of watertable rises, λ_T, and the mean rate of watertable decrease in time, η_T, whereas α_T is the mean vertical jump with which the river oscillates. Root profiles of riparian plants found remarkable agreement with the Tron et al. (2014) model (Tron et al., 2015).

2.2. Root distribution model: two-dimensional description of plant roots profile

It is instructive to obtain the total biomass of fine roots, TB_{fr}, predicted by the model of Schwarz et al. (2013). This can be done by integrating Eq. (2) along the lateral distance and under the assumption that $a_0 > 5$ (in order to capture the contribution of both terms of the distribution):

$$TB_{fr} = \int_{\phi_t/2}^{d_M} 2\pi x D_{fr}(x)dx = \frac{(a_0 - 2.768)\mu\phi_t}{a_0}, \tag{9}$$

where the product $\mu\phi_t$ is the total number of fine roots, N_{fr} Schwarz et al. (2013).

An expression for the Root system Area, $RA(x)$ as a function of the radial distance x is derived as follows. By summing the areal contribution of all roots with diameters in the range $\phi_0 < \phi \le \phi_M(x)$ at a given distance, x, one obtains

$$RA(x) = \int_{\phi_0}^{\phi_M(x)} \frac{\pi\phi^2}{4} N(\phi, x)d\phi, \tag{10}$$

i.e.,

$$RA(x) = \int_{\phi_0}^{\phi_M(x)} \frac{\pi\phi^2}{4} D_{fr} \frac{ln(1+\phi_M) - ln(1+\phi)}{ln(1+\phi_M)} \left(\frac{\phi}{\phi_0}\right)^{\lambda_r} d\phi. \tag{11}$$

After some algebraic manipulation, the solution reads

$$RA(x) = \pi \frac{D_{fr}(x)\left(-(-\phi_0)^{-\lambda_r} B_z\left[-\phi_0, 4+\lambda_r, 0\right] + (-\phi_M(x))^{-\lambda_r}\left(\frac{\phi_M(x)}{\phi_0}\right)^{\lambda_r} B_z\left[-\phi_M(x), 4+\lambda_r, 0\right] + \phi_0^3\left(ln[1+\phi_0] - ln[1+\phi_M(x)]\right)\right)}{4(3+\lambda_r)ln[1+\phi_M(x)]}, \tag{12}$$

where $B_z[\cdot, \cdot, \cdot]$ is the incomplete Beta function (Abramowitz and Stegun, 1965). This function provides the total area of roots with a diameter ϕ in the range $\phi_0 < \phi \le \phi_M(x)$, as a function of the radial distance from the stem, x. From this quantity, the Root Area Ratio, widely used in the literature (Bischetti et al., 2007; Smit et al., 2013), could easily be calculated. Notice, that the contribution of fine roots is not taken into account by this solution. In order to take fine roots into account in an approximate way one could extend the lower extreme of the integral term in (11) down to zero. Clearly, this operation is valid under the crude assumption that $N(x, \phi)$ provides a good estimates of the

number of fine roots for diameters $\phi < \phi_0$. Hence, one obtains

$$RA(x) = \int_0^{\phi_M(x)} \frac{\pi\phi^2}{4} D_{fr} \frac{ln(1+\phi_M) - ln(1+\phi)}{ln(1+\phi_M)} \left(\frac{\phi}{\phi_0}\right)^{\lambda_r} d\phi, \quad (13)$$

whose solution reads

$$RA(x) = \pi \frac{D_{fr}(x)\phi_M(x)^4 \left(\frac{\phi_M(x)}{\phi_0}\right)^{\lambda_r} \Phi[-\phi_M(x), 1, 4+\lambda_r]}{4(3+\lambda_r) ln[1+\phi_M(x)]}, \quad (14)$$

where, $\Phi[\cdot, \cdot, \cdot]$ is the Lerch transcendent function (Abramowitz and Stegun, 1965).

Next, one can proceed towards assembling the three models and use the models of Laio et al. (2006) and Tron et al. (2014) to redistribute the biomass along the vertical. For this, the pdf of the Tron et al. (2014) model's root profile, $R_T(z)$, must be obtained by operating the following transformation

$$r_T(z) = \frac{R_T(z)}{\int_0^h R_T(z)dz}, \quad (15)$$

which ensures that $\int r_T(z)dz = 1$.

By combining the root distributions of Laio (2006) and of Tron et al. (2014) a more comprehensive modelling framework is built. The new model describes how roots develop in soil because of soil moisture changes induced by rainfall infiltration (piston flow) and watertable oscillations (i.e., either due to river water level fluctuations or to oscillations of the watertable). The density functions for $r_L(z)$ and $r_T(z)$ are first defined over a vertical domain $0 \le z \le h$ and then combined via a weighting coefficient w_L ranging between 0 and 1,

$$r(z) = w_L r_L(z)\Theta[h-z] + (1-w_L) r_T(z), \quad (16)$$

where $w_L = 0$ corresponds to the Tron et al. (2014) model whereas $w_L = 1$ corresponds to the model of Laio (2006). The coefficient w_L is intended to be the only calibration parameter of the Root Distribution Model (RDM) and its role will be discussed in Section 3.3. Notice, that whilst $r_L(z)$ is mathematically defined for $0 \le z > \infty$ due to the hypothesis of absence of deep aquifer in the Laio (2006) model, in the presence of an aquifer at the depth h, its actual domain is restricted to the lower boundary $z \le h$. This implies that $\int_0^h r_L(z)dz < 1$, i.e. the root profile of model (Laio et al., 2006) has lost part of the biomass that would be created due to deep rainfall infiltration. However, for the RDM, this assumption may reasonably be associated with the loss of biomass due to precipitation events that infiltrated down to a depth $z > h$ where roots cannot grow because the soil is fully saturated.

The function $r(z)$ is then transformed into a pdf using

$$p_r(z) = \frac{r(z)}{\int_0^h r(z)dz}, \quad (17)$$

which re-scales $p_r(z)$ to be in the range $0 \le p_r(z) \le 1$. The function $p_r(z)$ can now be used to redistribute the model of Schwarz et al. (2012) along the vertical axis z. The global distribution of fine roots thus becomes

$$D_{fr}(x,z) = \frac{p_r(z)\mu\phi_t}{2\pi d_M} \left(\frac{1}{5\phi_t}\left(0.7 + 0.3\frac{x}{5\phi_t}\right)\Theta[5\phi_t - x] + \frac{1}{x}\Theta[x - 5\phi_t]\right), \quad (18)$$

with a total biomass of fine roots at each depth z equal to

$$TB_{fr}(z) = p_r(z)\frac{(a_0 - 2.768)\mu\phi_t}{a_0}. \quad (19)$$

As a consequence, the distribution of the number of roots, N, is also a function of three variables, that is $N(x, \phi, z)$ as well as the density of fine roots and the Root Area function, which we denote therefore as $RA_{RDM}(x, z)$.

3. Results and discussion

3.1. Root geometry distributions and contribution of fine roots to the RA

After integration along the vertical, the RDM provides the basic statistics of the model of Schwarz et al. (2012). Whilst referring to the original publication for details, it is insightful to plot the density of fine roots, the distribution of the root diameters at a given distance, and the distribution of a given diameter at all distances. These quantities are shown in Fig. 2 and are important for depicting the root distribution for a vertical slice of soil as shown in Fig. 1. The density of fine roots (Fig. 2a) typically increases up to a given distance from the trunk and then decreases. The number of roots within each class diameter is a monotonically decreasing function of the diameter size (Fig. 2b). The maximum root diameter (not shown) decreases linearly with increasing the distance from the trunk. However, the distribution of roots of a given diameter (Fig. 2c) shows non monotonic behaviour, i.e., it reaches a maximum before decreasing to zero at the distance beyond which that diameter class ends.

The contribution of fine roots to the RA as a function of the distance from the trunk, x, is shown in dimensionless variables in Fig. 3. The RA decreases with increasing lateral distance because of the decrease (with x) in the maximum root diameter and therefore the associated distributions of root diameters (see Schwarz et al. (2012) for details). Whilst for small trunk diameter (ϕ_t) the difference between the two solutions (12) and (14) is considerable, this difference tends to vanish as ϕ_t increases. This indicates that for large trunk diameters the role of fine roots in defining the RA becomes negligible compared to the contribution of roots with diameters larger than ϕ_0. Consequently, for small diameters (e.g., $\phi_t < 100$ mm), the solution (12) might noticeably underestimate the actual RA (Fig. 3) and so the use of (14) is preferred. In Fig. 3, the relative effect of the branching length for the same trunk diameter is evident. Reducing the branching length generally increases the amount of root biomass and therefore increases the similarity between the two solutions.

3.2. Effects of climate and root-aquifer connectivity

Climate and soil parameters affect the model directly according to the structure of Laio (2006) and Tron et al. (2014) models, whilst they only indirectly affect the Schwarz et al. (2012) allometric model. The effect of climate is shown in Fig. 4 for a tree with a root system that is (i) disconnected from the watertable (Fig. 4a-c), (ii) weakly (Fig. 4d-f) and (iii) strongly connected to it (Fig. 4g-i). The corresponding model parameters are reported in Table 1. The Budyko index is used to show how the root structure is redistributed in the soil as the dryness increases. When the root system is disconnected from the aquifer (e.g., Figs. 4a-c), it is expected that moisture would be more readily available in the upper layers of the soil and so the root structure becomes shallower and concentrated in the top of the soil profile. Schenk and Jackson (2002b) and Schenk and Jackson (2002a) reported that trees growing in semi-arid environments tend to generally develop deeper roots accessing the groundwater table, which allows to overcome moisture shortages. However, Zanetti et al. (2015) observed that this behaviour may be soil texture dependent and reported an opposite behaviour for trees growing on dikes and with a texture comparable to the one used in our model (in terms of soil porosity). This would also be consistent with the strategy of non-phreatophytic vegetation species (e.g., *Nitraria tangutorum* and *Calligonum mongolicum*) of uptaking water from larger spatial areas (Shiqin et al., 2017). This is also in general agreement with other models, e.g., Guswa (2008). Guswa (2008) uses a marginal carbon cost/benefit approach for determining the optimal root development in the soil. The present model shows that the root biomass spreads laterally in order to increase water uptake efficiency (Cannon, 1949; Smit et al., 2013). Hence, for increasing dryness index there would be not sufficient water available for uptake from the soil so that the tree would develop a

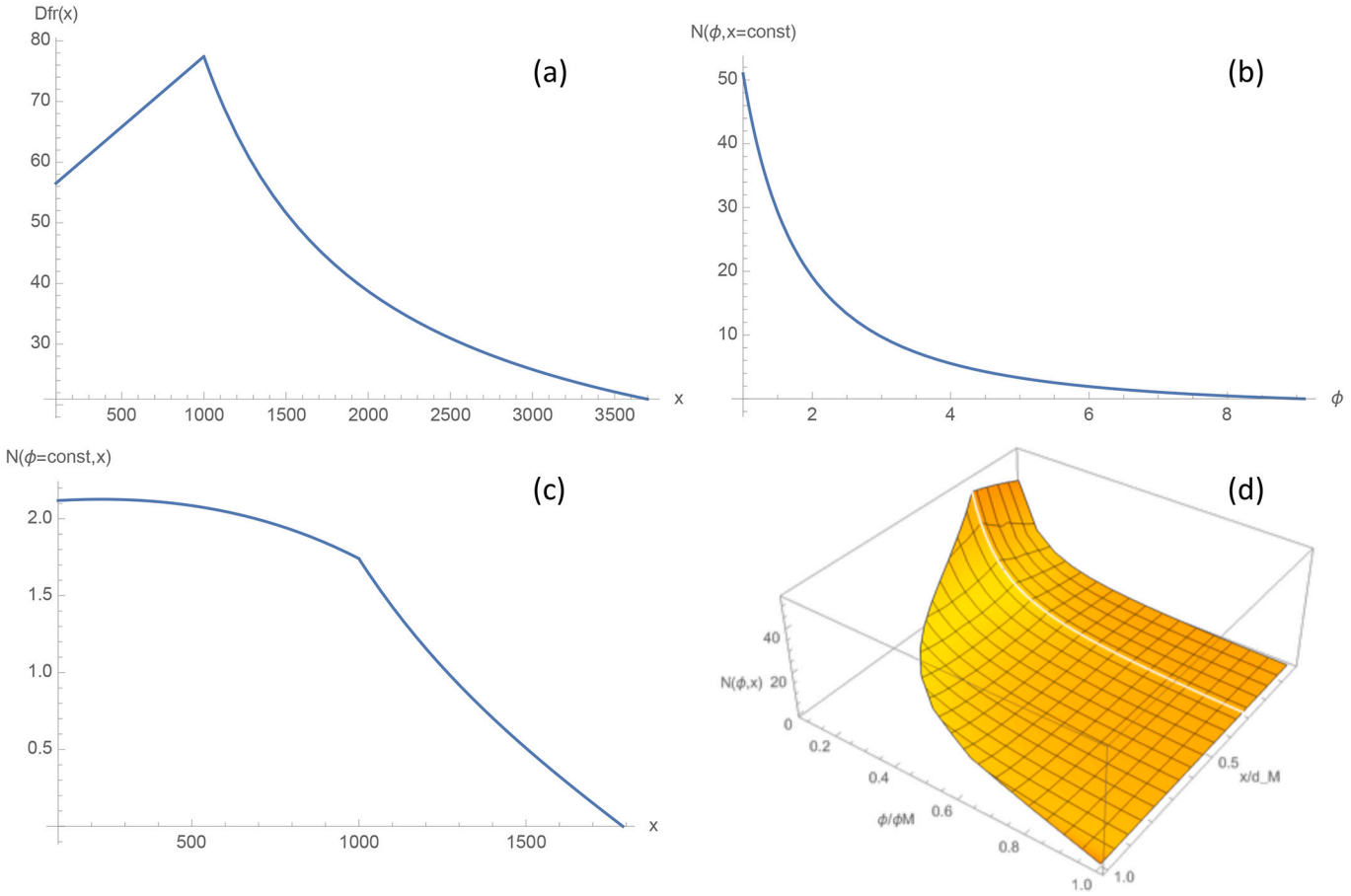

Fig. 2. Typical statistical distributions of the vertically integrated model (i.e., the Schwarz et al. (2012)) model generated with parameters $\phi_t = 200$ mm, $\mu = 9 \times 10^6$ roots/mm, $b = 90$ mm, $s = 0.36$ mm^{-1}, $a_0 = 18.5$. (a) Density of fine roots as a function of lateral distance; (b) number of roots per square metre of diameter ϕ (in mm) at a distance $x = 800$ mm from trunk; (c) number of roots per square metre with diameter $\phi = 6$ mm with distance; (d) 3D normalized plot of the root distribution $N(\phi, x)$.

root density distributions, which is generally higher closer to the soil surface and extend towards larger distances from the tree stem. The presence of an aquifer accessible by the roots may change this picture as hereafter discussed.

As far as the case of plants with roots directly connected to an aquifer is concerned, this can be taken into account by the model of Tron et al. (2014) as a constant -non-oscillating (or slowly oscillating) watertable located at a depth h from the soil surface (z in the model is directed downwards). This will limit plant root growth to a depth to $z \leq h$. Again, the amplitude L of the capillary fringe above the minimum river level where conditions are favourable for root water uptake and growth is generally well correlated to the sediment grain-size distribution (e.g., quantiles d_{90} and d_{10}).

In Figs. 4d-i, we show a few examples of spatial root distribution for a plant growing in a soil either weakly or highly connected to the aquifer. In both cases, the soil moisture availability depends both on precipitation and on aquifer fluctuations. The weakly connected case is characterized by a small capillary fringe amplitude that only reaches the deepest roots. On the contrary, the highly connected case entails a large capillary fringe amplitude that potentially oscillates up to the soil surface thus affecting the root structure over the entire profile. For the plant, connectivity is is related to a strategy that varies according to the plant species, i.e., from the physiological and phytological characteristics that make the plant able to allocate energy to the most efficient source of moisture.

The relevant model parameters are shown in Table 1. Figs. 4d-f show the case of a weakly connected aquifer characterized by a small ratio between the capillary fringe thickness and the aquifer depth to soil elevation, i.e. $L/h = 0.2$. In this environment roots are able to reach and uptake water from the capillary fringe, but are still predominantly influenced by the precipitation input. Interestingly, this situation can result in a bi-modal distribution of the RA. For example, when the groundwater level does not oscillate much in comparison with the rooting depth, then a small RA increase is already expected within the capillary fringe (Fig. 4d). If the aquifer oscillates slowly, then the amplitude of the oscillation affects the root density distribution. Because the capillary fringe recharges the soil moisture, the resulting RA distribution can become bi-modal. This effect is seen in larger sections of the soil profile as the mean magnitude of the (random) fluctuations increases, i.e., for larger α_T. The cases above are representative of plants growing on slopes in the vicinity of a water course that may slightly affect the position of the watertable. However, it is when the capillary fringe length, L, becomes comparable to the depth of the watertable, that the connectivity really increases. In this case, soil moisture availability is not limiting to plant growth throughout the soil profile, which therefore drives the water uptake. This is the case of riparian plants, whose root structure seems mainly be determined by water level oscillations due to the river hydrological regime (Tron et al., 2015; Pasquale et al., 2012). In this case, the root profile may deepen and show different shapes according to the water level fluctuation statistics. An interesting case is the inversion of the skewness of the root profile, which becomes negative, i.e., the distribution shows a deeper mode. As an example, Figs. 4g-i show the effect of the fluctuation magnitude for the case $L/h = 0.5$.

The maximal depth h of the watertable acts as a measurable

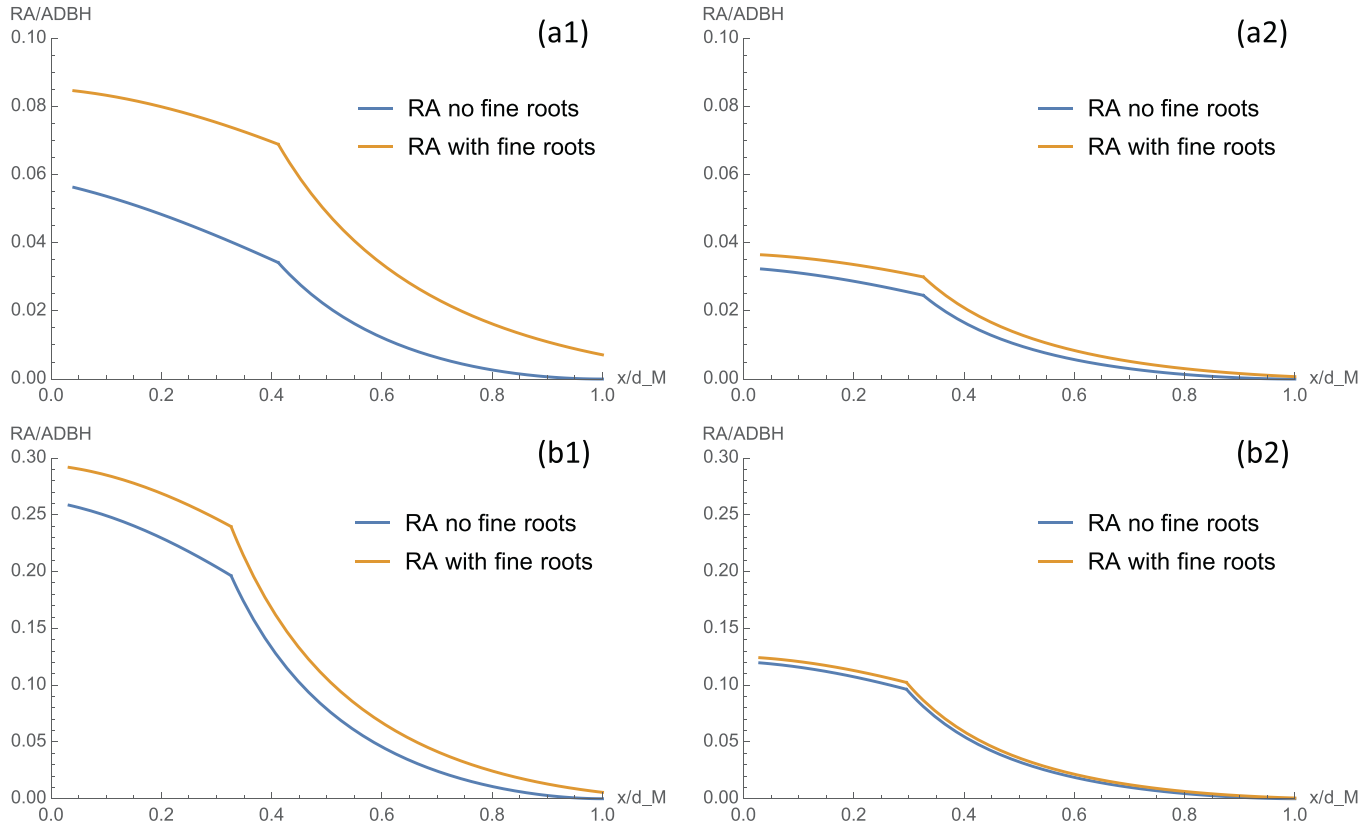

Fig. 3. $RA(x)$ normalized to the trunk area at DBH computed for a DBH, $\phi_t = 50$ mm, and branching length $b = 90$ mm (a1), $\phi_t = 100$ mm and $b = 90$ mm (a2), $\phi_t = 50$ mm and $b = 45$ mm (b1) and $\phi_t = 100$ mm and $b = 45$ mm (b2).

adjustable parameter that can be assessed at each distance from the main channel in order to simulate the presence of an aquifer at a certain depth. In practice, one could also make the relative frequency $\widetilde{\lambda}_T$ and the mean amplitude of the oscillations α_T functions of the distance from the river channel in order to simulate the potential reduction in the frequency of capillary fringe oscillations above h, although they are expected to remain (weakly) correlated to river fluctuations. In this case, without any precipitation and for a non-oscillating capillary fringe, the model would predict that plants develop a rectangular root profile of amplitude equal to L above h.

3.3. Role of the weighting parameter w_L

The parameter w_L is technically the only fitting parameter of RDM. However, because the level of connectivity of a plant with the aquifer also depends on plant species' strategy for water uptake from one or another source, w_L is actually expected to correlate with plant species characteristics. Regardless, w_L can easily be calibrated from the available data. Unfortunately, it is difficult to find complete sets of hydrometeorological, soil, groundwater and root data for a specific site, which precludes the validation of RDM for the time being. Indeed, while root excavation is technically easy to plan and conduct, a critical issue is to find locations where also long-enough records of groundwater and hydrometeorological variables that allow to estimate the parameters of the stochastic modelling components are simultaneously. In the following, we therefore advance a gross sensitivity analysis that demonstrates the effect of w_L on the vertical distribution function, $p_r(z)$ namely Eq. (17). This is shown in Fig. 5 for the cases of weak and high connectivity described in Fig. 4e,h. Notice that although the shape of the function $p_r(z)$ resembles the vertical shape of the RA, the two forms are not the same. This is due to the modulating effect that $p_r(z)$ has on the root quantities being plotted. This is particularly evident when comparing the RA profile (for equal RA) of Fig. 4h with the form of the redistribution function shown in Fig. 5b. Similarly, the comparison between Fig. 4e and Fig. 5a shows that $p_r(z)$ shifts the maximum of RA towards deeper depths so that the position of the maximum for the two functions does not coincide. RDM contains almost all physically based parameters except w_L, and should therefore be easy to calibrate provided that joint information about root (e.g., the RA and the allometric parameters of Schwarz et al. (2012) models) and environmental variables are available. Hence, from an practical point of view the fitting of $p_r(z)$ should be done indirectly via one of the available measured root quantities. Then, as w_L appears as a weighting coefficient of highly nonlinear functions, its calibration does not require particular tools and can be done with relatively few observations.

4. Conclusions

By assembling three root profile and distribution models from the literature, we built the Root Distribution Model, a unique framework that describes the expected spatial distribution of some typically used root system variables, including the RA. An alternative variable that is widely used in the literature is the closely related Root Area Ratio, which could be easily obtained from RA.

The main characteristic of the coupled model is that it models the spatial variability of tree root variables (i.e., along a radial distance from the main stem and as a function of the vertical depth) that are typically used in plant root quantification analysis (e.g., RA, spatial distribution of specific root diameters, distribution of root diameters at a specific location, maximum root diameter at a specific location, number of roots and density of fine-root.). The model can well represent the effect of different climatic conditions described by the Budyko index where the evaporative demand interplays with total precipitation. For example, in

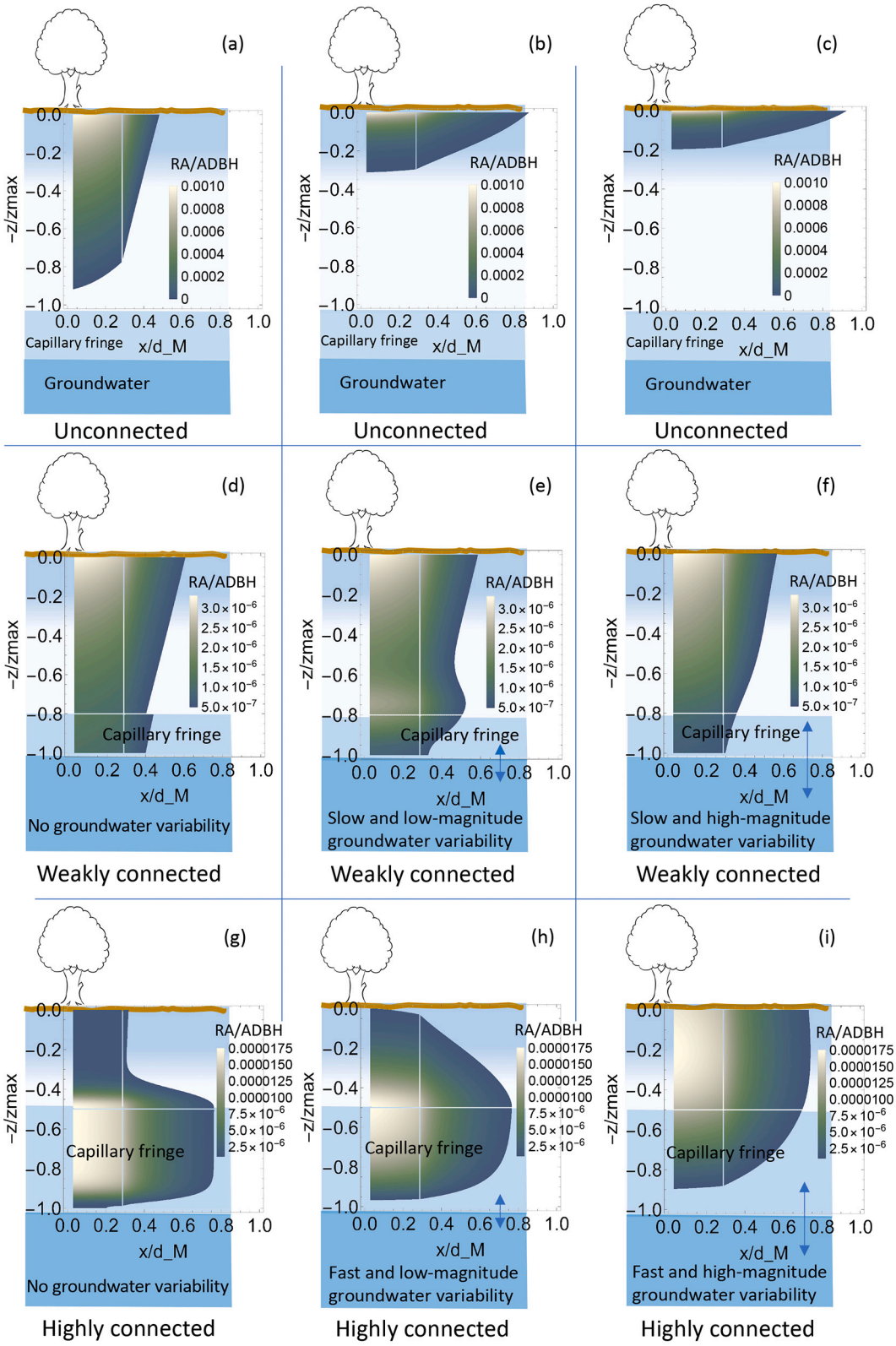

Fig. 4. Density plot of the RA normalized to the trunk DBH area as a function of the normalized horizontal distance x/d_M from the stem (in abscissas) and the normalized soil depth z/h (in ordinate). This collection of cases summarizes the effect of climate in terms of Budyko index, as well as the connection to static, slow and fast varying groundwater oscillations of different amplitude. The below-ground biomass is exaggerated compared to tree size for the sake of readability.

Table 1
Model parameters used for the simulations shown in Fig. 4. Fixed parameters for all simulations: $\phi_t = 300$ mm, $\phi_0 = 1$ mm, $\mu = 9 \times 10^6$ roots/mm, $b = 90$ mm, $s = 0.36$ mm^{-1}, $\lambda_r = -1$, $a_0 = 18.5$, $\lambda_p = 0.1$ d^{-1}, $\gamma_p = 10$ mm, $s_{fc} = 0.65$, $s_w = 0.2$.

Figure panel	(a)	(b)	(c)	(d)	(e)	(f)	(g)	(h)	(i)
Parameter	Unconnected			Weakly connected			Highly connected		
D_I	1.01	1.1	1.2	1.01	1.01	1.01	1.01	1.01	1.01
h	5000	5000	5000	5000	5000	5000	1000	1000	1000
α_T	$<10^{-2}$	$<10^{-2}$	$<10^{-2}$	$<10^{-2}$	200	1500	<20	100	500
η_T	–	–	–	0.0025	0.0025	0.0025	0.0025	0.1	0.1
$\widetilde{\lambda}_T = \lambda_T/\eta_T$	–	–	–	0.004	4	4	2	2	2
w_L	1	1	1	0.9	0.9	0.9	0.2	0.2	0.2

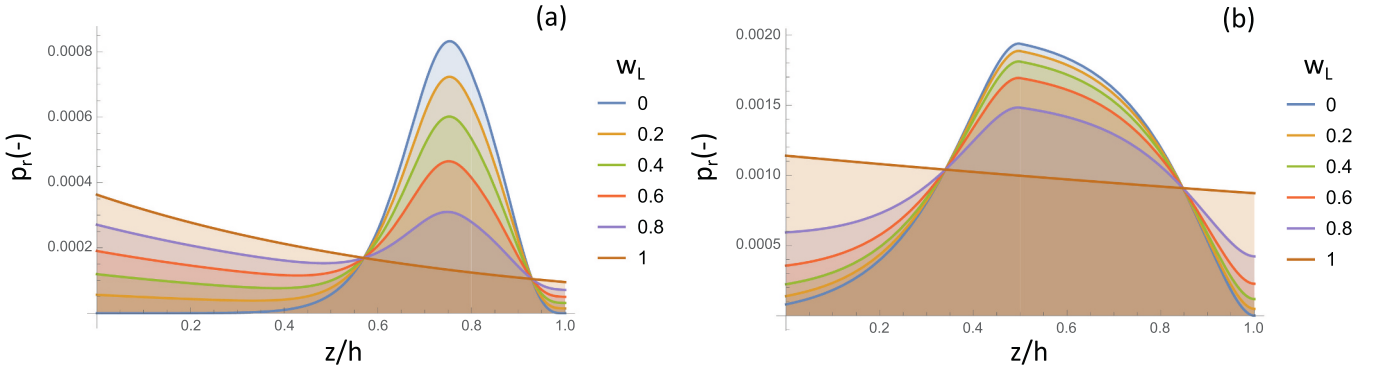

Fig. 5. Effect of the weighting parameter w_L on the shape of the vertical redistribution function $p_r(z)$ normalized at the maximum rooting depth imposed by the saturated watertable at a depth h. Panel (a) and (b) correspond to the parameters used in Fig. 4e and h, respectively.

dry climates and in the absence of connectivity with a deep aquifer, the expected RA becomes shallower and spread over larger distances from the main stem than in moderately humid environments. On the contrary, the connectivity to a deep aquifer changes this picture and reproduces root biomass plasticity characteristics (e.g., bi-modality for efficient water uptake both from rainfall input and the aquifer) that depend on soil properties, the degree of connectivity and the aquifer temporal dynamics.

Declaration of Competing Interest

The authors declare that they have no known competing financial interests or personal relationships that could have appeared to influence the work reported in this paper.

Data availability

No data was used for the research described in the article.

References

Abernethy, B., Rutherfurd, I.D., 2001. The distribution and strength of riparian tree roots in relation to riverbank reinforcement. Hydrol. Process. 15, 63–79.

Abramowitz, M., Stegun, I.A., 1965. Handbook of Mathematical Functions: With Formulas, Graphs and Mathematical Tables. Dover, New York.

Bischetti, G.B., Chiaradia, E.A., Simonato, T., Speziali, B., Vitali, B., Vullo, P., Zocco, A., 2007. Root strength and root area ratio of forest species in Lombardy (Northern Italy). In: Eco-and Ground Bio-Engineering: The Use of Vegetation to Improve Slope Stability. Springer, pp. 31–41.

Camporeale, C., Perucca, E., Ridolfi, L., Gurnell, A., 2013. Modeling the interaction between river morphodynamics and riparian vegetation. Rev. Geophys. 51, 1–36.

Cannon, W.A., 1949. A tentative classification of root systems. Ecology 30, 542–548.

Dingman, S.L., 2002. Physical Hydrology. Prentice Hall, New Jersey.

Edmaier, K., Burlando, P., Perona, P., 2011. Mechanisms of vegetation uprooting by flow in alluvial non-cohesive sediment. Hydrol. Earth Syst. Sci. 15, 1615–1627.

Edmaier, K., Crouzy, B., Perona, P., 2015. Experimental characterization of vegetation uprooting by flow. J. Geophys. Res. Biogeosci. 120, 1812–1824.

Ennos, A., Pellerin, S., 2000. Plant anchorage. In: Root Methods. Springer, pp. 545–565.

Gasser, E., 2020. The Relationship between Vegetation and Channel Processes Leading to the Recruitment of Large Wood in Mountain Catchments. Ph.D. thesis.. University of Natural Resources and Life Sciences (BOKU), Vienna.

Gasser, E., Schwarz, M., Simon, A., Perona, P., Phillips, C., Hubl, J., Dorren, L., 2019. A review of modeling the effects of vegetation on large wood recruitment processes in mountain catchments. Earth Sci. Rev. 194, 350–373.

Gasser, E., Perona, P., Dorren, L., Phillips, C., Hubl, J., Schwarz, M., 2020. A new framework to model hydraulic bank erosion considering the effects of roots. Water 12, 893–905.

Guswa, A.J., 2008. The influence of climate on root depth: a carbon cost-benefit analysis. Water Resour. Res. 44, w02427.

Laio, F., 2006. A vertically extended stochastic model of soil moisture in the root zone. Water Resour. Res. 42, W02406. https://doi.org/10.1029/2005WR004502.

Laio, F., D'Odorico, P., Ridolfi, L., 2006. Analytical model to relate the vertical root distribution to climate and soil properties. Geophys. Res. Lett. 33, L18401.

Pasquale, N., Perona, P., Francis, R., Burlando, P., 2012. Effects of streamflow variability on the vertical root density distribution of willow cutting experiments. Ecol. Eng. 40, 167–172.

Perona, P., Crouzy, B., 2018. Resilience of riverbed vegetation to uprooting by flow. Proc. Royal Soc. A Math. Phys. Eng. Sci. 474, 20170547.

Pollen-Bankhead, N., Simon, A., 2009. Enhanced application of root- reinforcement algorithms for bank-stability modeling. Earth Surf. Process. Landf. 34, 471–480.

Postma, J., Kuppe, C., Owen, M., Mellor, N., Griffiths, M., Bennet, M., Lynch, J.M., 2017. Opensimroot: widening the scope and application of root architectural models. New Phytol. 215, 1274–1286.

Reubens, B., Poesen, J., Danjon, F., Geudens, G., Muys, B., 2007. The role of fine and coarse roots in shallow slope stability and soil erosion control with a focus on root system architecture: a review. Trees 21, 385–402.

Ridolfi, L., D'Odorico, P., Laio, F., 2011. Noise-Induced Phenomena in the Environmental Sciences. Cambridge University Press.

Rodrigez-Iturbe, I., Porporato, A., 2005. Ecohydrology of Water Controlled Ecosystems. CUP, Cambridge.

Ruiz-Villanueva, V., WyZga, B., Zawiejska, J., Mikus, P., Hajdukiewicz, H., Hajdukiewicz, M., Stoffel, M., 2016. Large wood transport, deposition and remobilization during floods in the Czarny Dunajec River: Outcomes from numerical modelling. In: Flood Risk in the Upper Vistula Basin. Springer, pp. 103–125.

Schalko, I., Schmoker, L., Weitbrecht, V., Boes, R.M., 2020. Laboratory study on wood accumulation probability at bridge piers. J. Hydraul. Res. 58, 566–581.

Schenk, H.J., Jackson, R.B., 2002a. The global biogeography of roots. Ecol. Monogr. 72, 311–328. https://doi.org/10.1890/0012-9615(2002)072[0311:TGB0R]2.0.CO;2.

Schenk, H.J., Jackson, R.B., 2002b. Rooting depths, lateral root spreads and below-ground/above-ground allometries of plants in water-limited ecosystems. J. Ecol. 90, 480–494.

Schwarz, M., Lehmann, P., Or, D., 2010a. Quantifying lateral root reinforcement in steep slopes-from a bundle of roots to tree stands. Earth Surf. Process. Landf. 35, 354–367.

Schwarz, M., Preti, F., Giadrossich, F., Lehmann, P., Or, D., 2010b. Quantifying the role of vegetation in slope stability: a case study in Tuscany (Italy). Ecol. Eng. 36, 285–291.
Schwarz, M., Cohen, D., Or, D., 2012. Spatial characterization of root reinforcement at stand scale: Theory and case study. Geomorphology 171-172, 190–200.
Schwarz, M., Giadrossich, F., Cohen, D., 2013. Modeling root reinforcement using a root-failure Weibull survival function. Hydrol. Earth Syst. Sci. 17, 4367–4377.
Shiqin, X., Xibin, J., Bowen, J., Zhang, J., 2017. Root distribution of three dominant desert shrubs and their water uptake dynamics. J. Plant Ecol. 10, 780–790.
Smit, A.L., Bengough, A.G., Engels, C., van Noordwijk, M., Pellerin, S., van de Geijn, S.C., 2013. Root Methods: A Handbook. Springer Science & Business Media.
Smith, F.A., 2007. Plant Roots. Growth, Activity and Interaction with Soils.
Stokes, A., 2002. Biomechanics of tree roots anchorage. Marcel Dekker Chapter 2, 175–186.
Thorne, C.R., 1990. Effects of Vegetation on Riverbank Erosion and Stability. In: Thornes, J.B. (Ed.), Vegetation and Erosion. Wiley, Chichester, England, pp. 125–144.
Tron, S., Laio, F., Ridolfi, L., 2014. Effect of water table fluctuations on phreato- phytic root distribution. J. Theor. Biol. 360, 102–108.
Tron, S., Perona, P., Gorla, L., Schwarz, M., Laio, F., Ridolfi, L., 2015. The signature of randomness in riparian plant root distributions. Geophys. Res. Lett. 42, 7098–7106.
Wohl, E., Scott, D.N., 2017. Wood and sediment storage and dynamics in river corridors. Earth Surf. Process. Landf. 42, 5–23.
Zanetti, C., Vennetier, M., Mériaux, P., Provensal, M., 2015. Plasticity of tree root system structure in contrasting soil materials and environmental conditions. Plant Soil 387, 21–35.